NATURE, *399, 558-560, 10 June 1999*

# Detection of an impact-generated dust cloud around Ganymede

**Harald Krüger, Alexander V. Krivov*, Douglas P. Hamilton†, Eberhard Grün**

Max-Planck-Institut für Kernphysik, Postfach 103980, 69029 Heidelberg, Germany

∗ Astronomical Institute, St. Petersburg University, 198904 St. Petersburg, Russia

† University of Maryland, College Park, MD 20742-2421, USA

**Dust is ubiquitous in the solar system, being especially concentrated in the Zodiacal cloud and in the ornate ring systems surrounding the giant planets. Individual dust grains in each of these environments are thought to be generated by impact ejection from larger parent bodies, but until now no direct measurements of this important physical process have been made. Here we report on the first in-situ detections of a significant amount of sub-micrometre dust within a few radii of Jupiter's massive icy satellite Ganymede. Measurements of impact directions, impact speeds, and the mass distribution of the dust indicate that the dusty material emanates from Ganymede, and the data are consistent with secondary ejecta kicked off the moon's surface by the hypervelocity impacts of interplanetary dust. Enhanced dust fluxes near Callisto and Europa suggest that these icy satellites are also good sources of dusty debris.**

The Galileo spacecraft, orbiting Jupiter since 7 December 1995, is equipped with an impact ionisation dust detector [1] [2], which measures the plasma cloud released upon impact of submicrometre and micrometre dust particles onto its sensor. Masses and impact speeds of the grains are determined from the measured amplitudes and rise times of the impact charge signals on three channels [3]. Each impact event is classified into one of four quality classes, with class 3 being dust impacts and class 0 being noise. Depending on the noise rate of the charge measurements on the individual channels, classes 1 and 2 can be true dust impacts or noise events [3] [4]. Since class 2 events were relatively noise-free during the Ganymede flybys, here we analyse the combined class 2 and class 3 data set.

During close flybys of the Galilean moons, the overall impact rate of dust grains measured by the dust sensor showed a sharp peak within about half an hour centered on closest approach to each satellite [5] [6] [7]. Concentrations of dust were observed for Europa, Ganymede, and Callisto, with the Ganymede data set being the most complete; during the combined primary and Galileo Europa Mission (GEM), Galileo had four close flybys at Ganymede, and no further encounters with this satellite are planned in the future. The times of the Ganymede flybys are given in Tab. 1, and the geometry of the Galileo dust detections is explained in Fig. 1.

The direction in which the sensor was pointing during dust impacts (rotation angle, $\Theta$) at the Ganymede encounters is shown in Fig. 2. During the first three encounters (G1, G2 and G7) particles with $180° \leq \Theta < 360°$ were detected at altitudes below $4\,R_G$ (Ganymede radius, $R_G = 2,635$ km) and were concentrated towards Ganymede. Particles recorded from the opposite direction ($0° \leq \Theta < 180°$) did not show such a concentration [6].

Analysis of the velocity vector of Ganymede relative to Galileo, taking into account the 140° field of view of the dust detector [1], shows that particles belonging to a dust cloud around Ganymede could be detected with $\Theta = 270° \pm 90°$ during all four encounters. Thus, particles with $180° \lesssim \Theta \lesssim 360°$ detected during the first three flybys are compatible with having a Ganymede origin. We will call them Ganymede particles. Particles detected from the opposite direction ($0° \leq \Theta < 180°$) are streams of ten-nanometre dust grains [8] [9] which probably originate from Io [6] [7] [10]. They are not considered here.

Thirty-five Ganymede particles have been identified from the first three encounters purely by their impact direction (Tab. 1). The measured impact speeds of most Ganymede particles from these encounters are below 10 $\mathrm{km\,s^{-1}}$ with a mean value of $7.0 \pm 4.8$ $\mathrm{km\,s^{-1}}$ [11]. The stream particles, by contrast, have typical impact speeds as derived from the instrument's calibration which are much higher than 10 $\mathrm{km\,s^{-1}}$. Although the instrument calibration probably significantly underestimates the true speeds of the tiny dust stream particles [12], the calibrated impact speeds can be used to separate Ganymede particles from the dust streams (lowest panel of Fig. 2). The measured impact speeds of Ganymede particles agree well with the expected impact speeds for debris moving with Ganymede, $\sim 8$ $\mathrm{km\,s^{-1}}$ for all encounters, which suggests that these grains do indeed originate from Ganymede.

During Galileo's fourth Ganymede flyby (G8), both dust streams and Ganymede particles approached the sensor from the same direction ($180° \leq \Theta < 360°$). Based on data from the first three encounters, we adopt the following two criteria to separate Ganymede particles from dust streams: 1) Ganymede particles must be within $5\,R_G$ of the satellite and 2) The measured impact speed must be less than $10\,\mathrm{km\,s^{-1}}$. Nine particles satisfy these criteria (Tab. 1).

To characterise the dust cloud of Ganymede, we derived both mass and spatial distributions for the detected grains. The slope of the cumulative mass distribution for particles in the mass range $10^{-16}\,\mathrm{kg} \leq \mathrm{M} \leq 10^{-13}\,\mathrm{kg}$ is $\alpha = 0.98 \pm 0.06$ [11]. This is consistent with the typical slopes one expects for ejecta ($0.5 \lesssim \alpha \lesssim 1.0$ [13][14]). The spatial distribution of the dust grains is shown in Fig. 3. During the first three encounters (G1, G2 and G7) the number density increases towards Ganymede, with power law slopes ranging between -0.43 and -2.85. For the G8 encounter, no concentration of particles towards Ganymede is seen, perhaps due to uncertainties imposed by the separation from the stream particles and the large correction for incomplete transmission. The concentration of dust towards Ganymede leaves no doubt that the satellite itself is the source, since its gravitational and electromagnetic forces are too weak to appreciably focus interplanetary and/or interstellar dust. Since there are no indications for geysers or volcanoes on Ganymede, the most likely source is the continuous ejection of debris via bombardment of Ganymede's surface by interplanetary micrometeoroids.

In Figure 3, we combine the data from all four Ganymede flybys on a single plot. In interpreting the plot, we make two implicit assumptions, namely that the flux of dust released from Ganymede is constant in time and is constant over the satellite's surface. These assumptions, are probably not entirely true, but are accurate enough to allow simple order-of-magnitude estimates to be made. Most ejecta grains follow ballistic trajectories and reimpact Ganymede within several hours to a few days. These short-lived but continuously-replenished grains form a tenuous steady-state debris cloud which entirely envelopes Ganymede. Our measurements suggest a surprisingly large amount of orbiting ejecta in Ganymede's debris cloud: a steady-state value of roughly ten tons with a factor of 10 uncertainty.

The solid curve in Fig. 3 shows the predictions of an impact ejecta model [15] [16] [11], in which the interplanetary dust particles strike the surface of Ganymede, ejecting secondary particles. After choosing plausible values for the interplanetary micrometeoroids flux and the physical properties of Ganymede's surface, we find that the model predictions fit the dust data reasonably well.

Thus, our measurements and dynamical modelling strongly suggest that the dusty debris near Ganymede is produced by a continuous hail of interplanetary particles which strike the moon with enough energy to accelerate dusty debris off its surface. Similar clouds probably surround Europa and Callisto and, indeed, any satellite that lacks a gaseous atmosphere. The few previous attempts to directly detect dust close to satellites, most notably near the Moon [17], have led to inconclusive results. Our successful detection of dust in the vicinity of the large Jovian satellites underscores the general nature of the process and, in an ironic example of comparative planetology, provides strong support that our own Moon is a source of dust in near-terrestrial space.

A tiny fraction of impact debris is ejected at speeds sufficient to escape from Ganymede entirely. This material goes into orbit around Jupiter and will eventually be swept up by one of the Galilean satellites — these grains are probably responsible for some of the impact events detected by the dust instrument in the inner Jovian system [5] [6]. Unfortunately, the ring of material formed by these grains escaping from Ganymede is far too tenuous to be detected optically. However, the fraction of debris escaping a satellite is a steeply decreasing function of satellite mass, so steep that despite their reduced cross sections, small moons may be better sources of dust than large satellites [18]. This is most clearly exemplified in the new images of the Jovian ring provided by Galileo. The images show that the two tiny innermost moons, Adrastea and Metis, are sources for the main Jovian ring and dusty halo, while Thebe and Amalthea each give rise to a faint outer gossamer ring of dusty material [19][20]. Medium-sized satellites can also produce detectable rings: at Saturn the moon Enceladus supplies material to the broad and tenuous E ring [21] which, nevertheless, is substantial enough to be visible to ground-based telescopes. Impact ejection of dusty debris is likely to be important for explaining the distinctive black-white asymmetry of Saturn's moon Iapetus[22], for transporting exogenous material to Titan [23][22], and for producing dust in the Uranian[24] and Neptunian ring systems[25].

Future spacecraft measurements near satellites will quantify this important dust production mechanism, and will provide critical insight into the impact genesis of dusty rings. The next spacecraft likely to make in-situ measurements of impact-generated grains is Nozomi (formerly called Planet-B). It will attempt to detect dust belts around Mars, which are predicted to originate from impacts onto Phobos and Deimos [26][27]. In mid 2004, the Cassini spacecraft will arrive at Saturn. Cassini, which is equipped with an improved version of the Galileo dust instrument, will make numerous passes near the Saturnian satellites and will fly through the tenuous E ring, thereby sampling both the bound and escaping components of Enceladus ejecta.

# References


[1] Grün, E. et al., The Galileo Dust Detector. *Space Sci. Rev.* **60**, 317-340, (1992).

[2] Grün, E. et al., The Ulysses dust experiment. *Astron. Astrophys. Suppl. Ser.* **92**, 411-423, (1992).

[3] Grün, E. et al., Reduction of Galileo and Ulysses dust data. *Planet. Space Sci.* **43**, 941-951, (1995).

[4] Krüger, H., et al., Three years of Galileo dust data: II. 1993 to 1995. *Planet. Space Sci.*, **47**, 85-106, (1999).

[5] Grün, E. et al., Dust measurements in the jovian magnetosphere. *Geophys. Res. Lett.* **24**, 2171-2174, (1997).

[6] Grün, E. et al., Galileo Observes Electromagnetically Coupled Dust in the Jovian Magnetosphere. *J. Geophys. Res.*, **103**, 20011-20022, (1998).

[7] Krüger, H., Grün, E., Graps, A. and Lammers, S. Observations of electromagnetically coupled dust in the Jovian magnetosphere, *Astrophys. and Space Sci.*, in press, (1998).

[8] Grün, E. et al., Discovery of jovian dust streams and interstellar grains by the Ulysses spacecraft. *Nature* **362**, 428-430, (1993).

[9] Grün, E. et al., Constraints from Galileo observations on the origin of jovian dust streams. *Nature* **381**, 395-398, (1996).

[10] Graps, A. L., Grün, E., Svedhem, H., Krüger, H., Horanyi, M., Heck, A. and Lammers, S., Jovian Dust Streams Origin Revealed, *Nature*, in preparation, (1999).

[11] Krüger, H., Krivov, A. V., Grün, E., Hamilton, D. P., A Dust Cloud of Ganymede Maintained by Hypervelocity Impacts of Micrometeoroids, *J. Geophys. Res.*, in prep., (1999).

[12] Zook, H. A., et al., Solar wind magnetic field bending of jovian dust trajectories. *Science* **274**, 1501-1503, (1996).

[13] Koschny, D. and Grün, E., Impacts into ice-silicate mixtures: Crater morphologies, volumes, depth-to-diameter ratios and yield. *Icarus*, submitted, (1996).

[14] Koschny, D. and Grün, E., Impacts into ice-silicate mixtures: Ejecta mass and size distributions. *Icarus*, submitted, (1996).

[15] Krivov, A. V., On the dust belts of Mars. *Astronomy and Astrophysics*, 291, 657–663, (1994).

[16] Krivov, A. V. and Jurewicz, A., The ethereal dust envelopes of the Martian moons. *Planet. Space Sci.*, 47, 45-56, (1999).

[17] Iglseder, H., Uesugi, K., and Svedhem, H., Cosmic dust measurements in lunar orbit. *Advances in Space Research*, **17(12)**, 177–182, (1996).

[18] Burns, J. A., Showalter, M. R., and Morfill, G. E., The ethereal rings of Jupiter and Saturn. In Greenberg, R. and Brahic, A., Eds., Planetary Rings, pp. 200–272. Univ. of Ariz. Press, Tucson, 1984.

[19] Ockert-Bell, M. E., et al., The structure of Jupiter's ring system as revealed by the Galileo imaging experiment. *Icarus*, submitted, (1998).

[20] Burns, J. A., Nicholson, P. D., Showalter, M. R., Hamilton, D. P., de Pater, I. and Bell, M., The formation of Jupiter's faint rings, *Science*, submitted, (1999).

[21] Hamilton, D. P. and Burns, J. A., Origin of Saturn's E ring: Self-sustained, naturally. *Science*, **264**, 550–553, (1994).

[22] Burns, J., Hamilton, D. P., Mignard, F., and Soter, S., The contamination of Iapetus by Phoebe dust. In Gustafson, B. A. S. and Hanner, M. S., Eds., Physics, Chemistry, and Dynamics of Interplanetary Dust (ASP Conf. Series, vol. 104), pp. 179–182. Kluwer, Dordrecht, (1996).

[23] Banaszkiewicz, M. and Krivov, A. V., Hyperion as a dust source in the saturnian system. *Icarus*, **129**, 289–303, (1997).

[24] Esposito, L.W., A. Brahic, J.A. Burns, and Marouf, E.A., Physical properties and origin of the Uranian rings. In J.T. Bergstrahl, E.A. Miner, and M.S. Matthews, Eds., Uranus, Univ. of Ariz. Press, Tucson, pp. 410-465, (1991).

[25] Colwell, J.E., and Esposito, L.W., A model of dust production in the Neptune ring system. *Geophys. Res. Let.* **17**, 1741-1744, (1990).

[26] Soter, S., The dust belts of Mars. Rept. CRSR No. **462**, 1971.

[27] Krivov, A. V. and Hamilton, D. P., Martian dust belts: Waiting for discovery. *Icarus*, **128**, 335–353, (1997).

# Tables

Table 1: **Satellite encounter characteristics and dust impact detections.** Galileo satellite flybys are labelled with the first letter of the Galilean satellite which was the encounter target during that orbit, followed by the orbit number (column 1). C/A = Closest Approach. Galileo's data transmission capability is very limited because its high-gain antenna failed to open completely. Although each impact event is counted, the full set of measured parameters (impact direction, impact charge, charge rise times, etc.) is not always transmitted to Earth. During the satellite encounters, the transmission rate was roughly one full impact parameter set per minute. The higher impact rates experienced during the G1, G2, and G8 encounters resulted in loss of some data. Because all impacts were counted, however, we can derive the true number of Ganymede particles (column 5) by multiplying the total number of impacts (from all directions) by the fraction of Ganymede particles for which we have full data sets (column 4) [11].

| Flyby | Time of C/A [year-day] | Altitude at C/A [km] | Particles with full data set | Corrected number of particles |
|---|---|---|---|---|
| (1) | (2) | (3) | (4) | (5) |
| G1 | 96-179.270 | 844 | 15 | 30 |
| G2 | 96-250.791 | 262 | 9 | 48 |
| G7 | 97-095.299 | 3095 | 11 | 11 |
| G8 | 97-127.665 | 1596 | 9* | 49 |

* Only particles with velocity $v \leq 10\ \mathrm{km\,s^{-1}}$ and below $5\,R_G$ altitude included.

# Figures

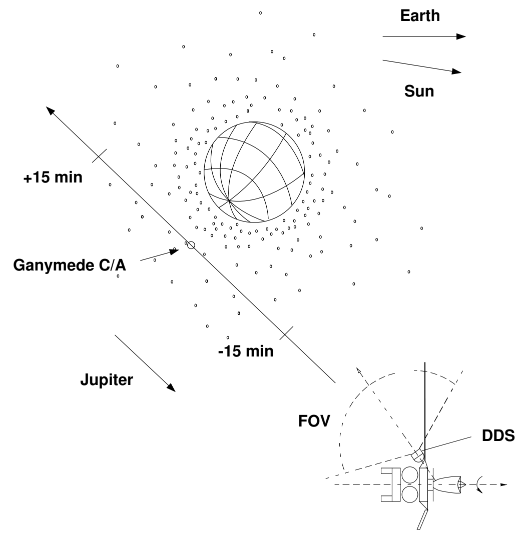


Figure 1: Galileo's trajectory and geometry of dust detection during the G7 Ganymede flyby. The Galileo spacecraft is sketched in an orientation it was in during the flyby: the antenna points towards Earth and the dust detector faces the anti-Earth hemisphere. The dust detector (DDS) has a conical field of view (FOV) of 140° and is mounted at an angle of 60° with respect to the positive spin-axis (anti-Earth direction). As Galileo spins about the spacecraft-Earth line, the dust detector axis sweeps out a cone with 120° opening angle, sampling dust arriving from different directions. Here, the dust detector is shown in an orientation where particles belonging to a cloud of dust from Ganymede can be detected (rotation angle $\Theta \sim 270°$). Dust stream particles approach from the opposite direction (Jupiter direction, $\Theta \sim 90°$).

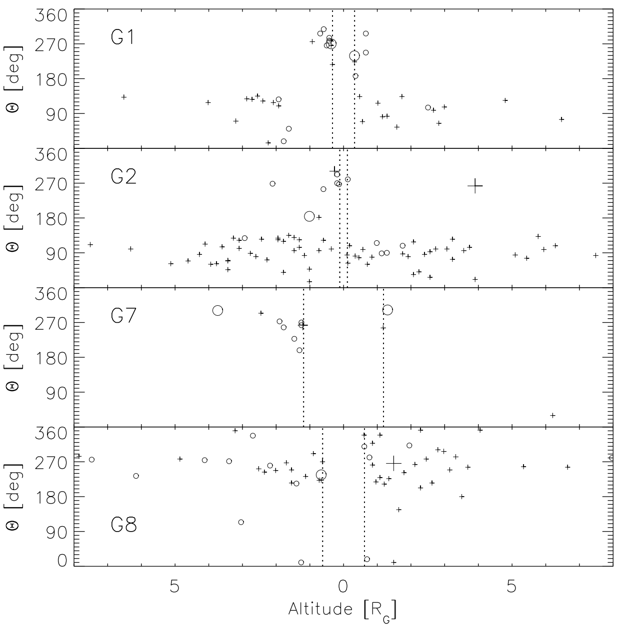


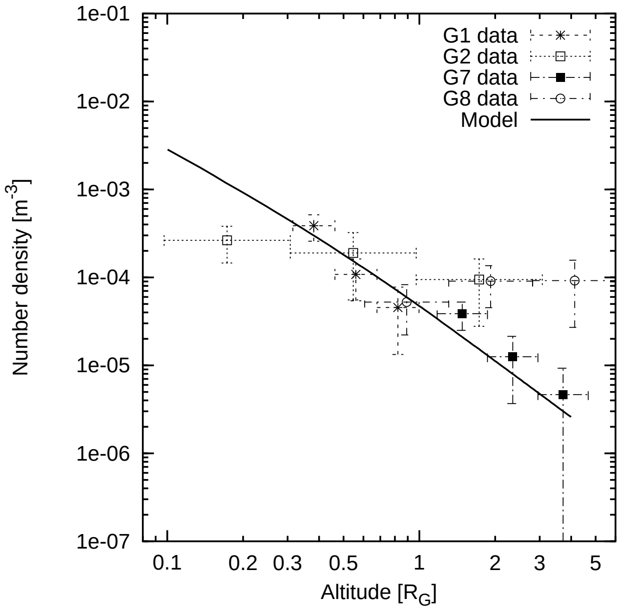


Figure 2: Sensor direction (rotation angle, $\Theta$) versus altitude of Galileo above the surface of Ganymede at the time of dust impact for all four Ganymede encounters. The altitude range shown corresponds to a time interval of 1.6 hours. At $\Theta = 0°$ the sensor axis points closest to ecliptic north, at 90° it points closest to the direction of Jupiter. The direction to Ganymede is about 270° during approach. Here we plot only impacts for which we have a complete set of parameters. The apparent concentration of these particles within $5\,\mathrm{R_G}$ is due to an increased data transmission rate near Ganymede. Circles show particles with impact speeds below $10\ \mathrm{km\,s^{-1}}$ and crosses show particles with higher speeds. The symbol sizes indicate the impact charge created by the particles ($10^{-14}\,\mathrm{C} \le \mathrm{Q_I} \le 10^{-11}\,\mathrm{C}$). Ganymede's radius is $\mathrm{R_G} = 2,635\,\mathrm{km}$. Galileo did not pass through the altitude ranges between the dotted lines. For G1, G2 and G7 Ganymede particles approached from the opposite direction ($180 < \Theta \le 360°$) than the stream particles ($0 < \Theta \le 180°$). In G8 both types of particles approached from the same direction and they can be separated by their impact speed only.

Figure 3: The number density of dust as a function of altitude above the surface of Ganymede. To obtain the number density from the data (symbols with error bars), we defined altitude bins equally spaced outward from Ganymede on a logarithmic scale (indicated by horizontal bars) and divided the number of particles for which the complete set of parameters has been transmitted to Earth in a given distance bin by the time Galileo has spent in this bin. We corrected for incomplete data transmission (Tab. 1) and divided the rates by the effective spin-averaged detector area to obtain fluxes in $[\mathrm{m^{-2}\,s^{-1}}]$. Finally, we divided the results by the mean impact velocity for a given flyby, which results in mean number densities $[\mathrm{m^{-3}}]$ in various bins. Vertical error bars reflect statistical errors due to the small number of impacts. The solid curve is the theoretical distribution of the impact ejecta expected for interplanetary impactors with a plausible set of model parameters [15] [16] [11].